Emergent Non-Fermi-Liquid at the Quantum Critical Point of a Topological Phase Transition in Two Dimensions

Hiroki Isobe, Bohm-Jung Yang, Andrey Chubukov, Jörg Schmalian, and Naoto Nagaosa

Phys. Rev. Lett. **116**, 076803 — Published 18 February 2016

DOI: 10.1103/PhysRevLett.116.076803

Emergent non-Fermi liquid at the quantum critical point of a topological phase transition in two dimensions

Hiroki Isobe,[1] Bohm-Jung Yang,[2,3,4] Andrey Chubukov,[5] Jörg Schmalian,[6] and Naoto Nagaosa[1,2]

[1]*Department of Applied Physics, University of Tokyo, Bunkyo, Tokyo 113-8656, Japan*
[2]*RIKEN Center for Emergence Matter Science (CEMS), Wako, Saitama 351-0198, Japan*
[3]*Center for Correlated Electron Systems, Institute for Basic Science (IBS), Seoul 151-747, Korea*
[4]*Department of Physics and Astronomy, Seoul National University, Seoul 151-747, Korea*
[5]*William I. Fine Theoretical Physics Institute and School of Physics and Astronomy, University of Minnesota, Minneapolis, MN 55455, USA*
[6]*Institutes for Theory of Condensed Matter and for Solid State Physics, Karlsruhe Institute of Technology, D-76131 Karlsruhe, Germany*

(Dated: January 14, 2016)

We study the effects of Coulomb interaction between 2D Weyl fermions with anisotropic dispersion which displays relativistic dynamics along one direction and non-relativistic dynamics along the other. Such a dispersion can be realized in phosphorene under electric field or strain, in TiO_2/VO_2 superlattices, and, more generally, at the quantum critical point between a nodal semimetal and an insulator in systems with a chiral symmetry. Using the one-loop renormalization group approach in combination with the large-N expansion, we find that the system displays interaction-driven non-Fermi liquid behavior in a wide range of intermediate frequencies and marginal Fermi liquid behavior at the smallest frequencies. In the non-Fermi liquid regime, the quasiparticle residue Z at energy E scales as $Z \propto E^a$ with $a > 0$, and the parameters of the fermionic dispersion acquire anomalous dimensions. In the marginal Fermi-liquid regime, $Z \propto (|\log E|)^{-b}$ with universal $b = 3/2$.

PACS numbers: 71.10.Hf, 73.43.Nq, 73.22.–f, 73.21.–b

Introduction. After the discovery of time-reversal invariant topological band insulators [1, 2], the notion of topological states of matters has been extended to a broad class of systems. Recent studies of three-dimensional (3D) Weyl and Dirac semimetals with two-fold and four-fold degeneracy, respectively, have demonstrated that these systems also possess quantized topological charges and associated topological surface states [3–11]. Since the topological invariant assigned to each nodal point guarantees its stability, the transition from a topological semimetal to an insulator can be achieved when pairs of nodal points with opposite topological charges merge at the same momentum [12]. The quantum critical point (QCP) of semimetal-insulator transitions should have emerging gapless degrees of freedom with zero topological charge [13, 14].

Because the topological charge of a nodal point is solely determined by the energy dispersion around it, the vanishing of a topological charge at a QCP implies that at this point the dispersion of low energy excitations must become unconventional. Indeed, it has recently been shown that a new type of fermionic excitations, dubbed a 3D anisotropic Weyl fermion (AWF), appears at the QCP between a 3D Weyl semimetal and an insulator [12–14]. A 3D AWF has an anisotropic energy dispersion, which is quadratic in one direction and linear in the other two orthogonal directions. Such a dispersion brings about highly unusual quantum critical behavior. Most notably, quantum fluctuations of 3D AWFs screen the long-range Coulomb interaction and make it anisotropic, however the long-ranged nature of the interaction is preserved. The screened anisotropic Coulomb potential becomes an irrelevant perturbation in the low-energy limit, i.e., low-energy fermions remain free quasiparticles [14]. Electron interaction effects in other anisotropic Weyl systems have also been studied [15, 16].

In this letter, we describe a semimetal-insulator transition and associated quantum criticality in a system of two-dimensional (2D) AWF with long-range Coulomb interaction. The role of the Coulomb interaction in 2D nodal semimetals $V(\boldsymbol{q}) \propto 1/|\boldsymbol{q}|$ has been widely studied with particular emphasis on graphene [17–20]. The conclusion is that at strong coupling, the Coulomb interaction generates anomalous exponents [20]. This behavior, however, holds only at intermediate frequencies because the dimensionless coupling flows towards smaller values, and below a certain energy the system necessary enters into a weak coupling regime. In this regime the renormalizations are only logarithmical (marginal) [19, 22–27], and the quasiparticle residue tends to a finite value at zero energy, i.e., at smallest frequencies graphene preserves Fermi-liquid behavior. As a consequence, interactions dress physical observables, like the optical conductivity, only by extra logarithmic factors [22, 23, 28, 29].

We argue that the behavior changes fundamentally when a semi-metal is brought to the quantum critical point of the semimetal-insulator transition, at which pairs of nodal points merge. In this case, the low energy excitations around a gapless point are 2D AWFs with linear dispersion in one direction and quadratic in the other [30–38], i.e., a 2D AWF displays relativistic and non-relativistic dynamics simultaneously.

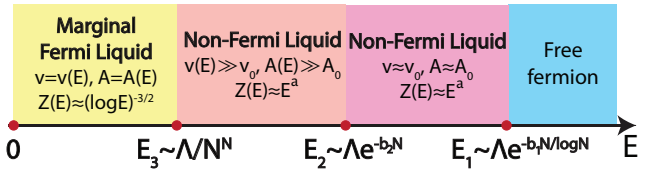

FIG. 1: (Color online) Evolution of quasiparticle properties as the energy scale varies. There are three energy scales $E_1 \sim \Lambda e^{-b_1 N/\log N}$, $E_2 \sim \Lambda e^{-b_2 N}$, and $E_3 \sim \Lambda/N^N$ characterizing each region. Here $b_{1,2}$ are constants of $O(1)$, and $v(E)$, $A(E)$, $Z(E)$ are the velocity, the inverse mass, and the quasiparticle residue, which are running as E decreases. Λ is of the order of the band width. The same sequence of phases also holds when the energy E is replaced by the temperature.

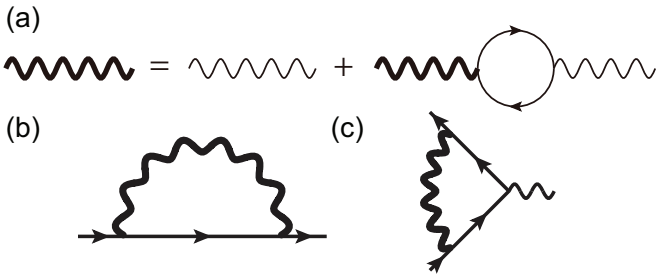

FIG. 2: (a) Feynman diagrams representing the RPA boson propagator (bold wavy line). Each fermion loop, accompanied by a factor N, is resummed in the boson propagator. (b) electron self-energy and (c) the vertex function.

We analyze the effects of Coulomb interaction in 2D AWFs by combining a renormalization group (RG) analysis and a large N expansion. We find (see Fig. 1) that over a wide range of energies the screened Coulomb interaction is a relevant perturbation, and the system is in the strong coupling limit and displays non-Fermi liquid behavior with power-law energy dependence of the quasiparticle residue $Z \propto E^a$, where $a = O((\log N)/N)$. This behavior starts at $E_1 \sim \Lambda e^{-b_1 N/\log N}$, where Λ is of the order of the bandwidth and $b_1 = O(1)$, and extends down to very low energy $E_3 \sim \Lambda/(N^N)$. In the subrange $E_3 < E < E_2 < E_1$, where $E_2 \sim \Lambda e^{-b_2 N}$, $b_2 = O(1)$, the parameters of the fermionic dispersion (the velocity and the effective mass) also become energy dependent and vary as powers of E with anomalous exponents $O(1/N)$. At even smaller energies $E < E_3$, the system crosses over to weak coupling behavior. However, contrary to the case of 2D nodal semimetals, 2D AWFs do not become free particles at the smallest frequencies. Instead, in the limit $E \to 0$, the system displays marginal Fermi liquid (MFL) behavior with universal, N-independent quasiparticle weight $Z(E) \propto (\log E)^{-3/2}$.

The model. Non-interacting 2D AWF are described by

$$H_0 = -A\partial_x^2 \tau_x - iv\partial_y \tau_y, \qquad (1)$$

where $1/(2A) > 0$ is the mass along x direction and v is the velocity along y direction. The Pauli matrices $\tau_{x,y}$ are used to denote the valence and conduction bands. The absence of τ_z in H_0 ensures that the Hamiltonian has a chiral symmetry, which guarantees the stability of AFW in 2D. The semimetal-insulator transition can be described by adding to H_0 a perturbation term $m\tau_x$ with a constant m. Depending on the sign of m, the system becomes either a gapped insulator ($m > 0$) or a semimetal ($m < 0$) with two nodal points on the k_x axis with the winding numbers ± 1, respectively. The distance between two nodal points decreases as $|m|$ is reduced, and at $m = 0$ two nodal points merge, resulting in a gapless point with a zero topological charge [30, 31]. The anisotropic dispersion leads to the density of states $\rho_{\rm QCP}(E) \propto \sqrt{E}$, which is obviously enhanced in the low energy limit as compared to the case of a semimetal for which $\rho_{\rm SM}(E) \propto E$. This suggests that interaction effects are most relevant at the QCP.

We consider long-range Coulomb interaction between 2D AWF. The corresponding effective action is

$$S = \int d\tau d^2x \psi_a^\dagger [(\partial_\tau + ig\phi) + H_0]\psi_a + \frac{1}{2}\int d\tau d^3x (\partial_i \phi)^2, \qquad (2)$$

where ψ_a describes a two-component fermion field with the subscript $a = 1, ..., N$ labeling the species of AWF, and ϕ is a bosonic field which one obtains via Hubbard-Stratonovich transformation of the instantaneous Coulomb potential. The subscript $i = x, y, z$ and the summation over repeated indices is implied. Observe that the bosonic field ϕ is defined in 3D space whereas the electron is confined to a 2D plane. Once the z-dependence of ϕ, is integrated out, the Coulomb potential in momentum space becomes $V(\boldsymbol{q}) \propto 1/|\boldsymbol{q}|$. The dimension-full boson-fermion coupling associated with Coulomb potential is $g = e/\sqrt{\varepsilon}$, where e is the electric charge and ε is determined by the dielectric constant. The corresponding dimensionless coupling α, which appears in perturbation theory, is the ratio of the Coulomb potential $E_c \sim A^{-1} v g^2$ and the electron kinetic energy $E_{\rm kin} \sim A^{-1} v^2$: $\alpha \equiv E_c/E_{\rm kin} = g^2/v$. To control the theory analytically, we extend the model to N fermionic flavors and consider the large N limit. At large N, the dimensionless coupling constant becomes $\alpha_N = N\alpha$.

Bosonic and fermionic propagators. We follow the same strategy as in earlier approaches on large N theories of quantum-critical behavior of itinerant fermions [20, 39] and compute fermionic and bosonic self-energies in a self-consistent scheme. Namely, we first compute the *one-loop* bosonic self-energy (bosonic polarization operator $\Pi_1(\Omega, \boldsymbol{q})$) as the latter contains N (and also, as we will see, contains smaller power of q_y compared to the bare term $D_0^{-1} = 2(q_x^2 + q_y^2)^{1/2}$), then use the dressed dynamical bosonic propagator $D_1^{-1}(\Omega, \boldsymbol{q}) = D_0^{-1}(\boldsymbol{q}) - N\Pi_1(\Omega, \boldsymbol{q})$ to compute the fermionic self-energy and corrections to the one-loop $\Pi_1(q, \Omega)$ within the $1/N$ expansion. We

show that the corrections depend logarithmically on the running energy and solve the RG equations for the full propagators using $1/N$ as a control parameter. Note that this approach is qualitatively different from direct perturbation theory in which one expands around the bare (unscreened) dispersion.

The evaluation of the one-loop polarization bubble is rather involved. We present the details in the Supplemental Material (SM) [40] and here list the result. We find that $\Pi_1(\Omega, \boldsymbol{q})$ can be well approximated by the interpolation formula

$$\Pi_1(\Omega, \boldsymbol{q}) = -\alpha \left[\frac{d_x A^{1/2} q_x^2}{\Delta(\Omega, \boldsymbol{q})^{1/4}} + \frac{d_y A^{-1/2} v^2 q_y^2}{\Delta(\Omega, \boldsymbol{q})^{3/4}} \right], \quad (3)$$

where $\Delta(\Omega, \boldsymbol{q}) = \Omega^2 + cA^2 q_x^4 + v^2 q_y^2$, and d_x, d_y, and c are constants, whose explicit values we present in SM. This $\Pi_1(\Omega, \boldsymbol{q})$ is numerically very close to the actual $\Pi_1(\Omega, \boldsymbol{q})$ for all parameters (see SM) and matches the exact results in the three limits: (i) $\Pi_1(\Omega = q_y = 0) = -\frac{g^2}{16v}|q_x|$, (ii) $\Pi_1(|\Omega| \gg Aq_x^2, q_y = 0) = -\frac{\alpha}{8\sqrt{\pi}} \frac{\Gamma(3/4)}{\Gamma(9/4)} \frac{\sqrt{A} q_x^2}{\sqrt{\Omega}}$, (iii) $\Pi_1(q_x = 0) = -\frac{\alpha}{6\sqrt{\pi}} \frac{\Gamma(5/4)}{\Gamma(3/4)} \frac{v^2 q_y^2/\sqrt{A}}{(\Omega^2 + v^2 q_y^2)^{3/4}}$. Observe that while $\Pi_1(\Omega = q_y = 0) \propto |q_x|$ has the same functional dependence as $D_0^{-1}(q_x) = |q_x|$, $\Pi_1(q_x = 0, \Omega \sim v q_y) \propto |q_y|^{1/2}$ is parametrically larger than $D_0^{-1}(q_y) = |q_y|$ at small q_y [41].

We now use the bosonic propagator with $\Pi_1(\Omega, \mathbf{q})$ included and compute the one-loop fermionic self-energy $\Sigma_1(\omega, \boldsymbol{k})$ and vertex correction δg_1. The corresponding diagrams are shown in Fig. 2. For the self-energy, we obtain at large $\alpha_N = Ng^2/v$ (see SM for details.)

$$\begin{aligned} \Sigma_1(\omega, \boldsymbol{k}) &= (-ig)^2 \int \frac{d\Omega d^2 q}{(2\pi)^3} G_0(\omega + \Omega, \boldsymbol{k} + \boldsymbol{q}) D(\Omega, \boldsymbol{q}) \\ &\equiv \Sigma_\omega \cdot i\omega - \Sigma_{k_x} \cdot A k_x^2 \tau_x - \Sigma_{k_y} \cdot v k_y \tau_y, \end{aligned} \quad (4)$$

where

$$\Sigma_\omega = \gamma_z l, \ \Sigma_{k_x} = \Sigma_\omega + \gamma_A l, \ \Sigma_{k_y} = \Sigma_\omega + \gamma_v l, \quad (5)$$

$l = \log(\Lambda/E)$, Λ is the upper energy cutoff, and E is the largest of $(|\omega|, v_F|k_y|, Ak_x^2)$. The parameters are $\gamma_z = \frac{\sqrt{15}}{\pi^{3/2}} (\log \alpha_N)/N$, $\gamma_A = 0.1261/N$, and $\gamma_v = 0.3625/N$. We see that the quasiparticle residue $Z = [1 + \partial\Sigma_1/\partial(i\omega)]^{-1}$ and the parameters of electronic dispersion acquire logarithmically singular $1/N$ corrections. Observe that the correction to Z is stronger than the corrections to v and A by $\log \alpha_N$.

For the vertex correction we find at vanishing external momentum and frequency

$$\delta g_1 = -g^2 \int \frac{d^3 k}{(2\pi)^3} D(k) G_0(k) G_0(k) \equiv \Sigma_\omega. \quad (6)$$

This is consistent with the Ward-Takahashi identity.

Renormalization group analysis. One can verify that higher-order corrections contain higher powers of l. To sum up the series of logarithms, we express the full self-energy $\Sigma(\omega, \boldsymbol{k})$, the full vertex g, and the full polarization bubble self-consistently, via full Green's functions and full vertices, and then represent $\Sigma(l)$, $g(l)$, and $\Pi(l)$ as integrals $\int^l dl'$ over running l', and obtain RG equations by taking derivatives with respect to the upper limit [44]. The RG equations for $Z(l)$, $v(l)$, and $A(l)$ are ($\dot{X} = dX/dl$)

$$\dot{Z}(l) = -\gamma_z(l) Z(l), \ \dot{v}(l) = \gamma_v v(l), \ \dot{A}(l) = \gamma_A A(l) \quad (7)$$

where $\gamma_z(l) = \gamma_z + \frac{\sqrt{15}}{\pi^{3/2}} \frac{1}{N} \log \frac{v}{v(l)}$. The product gZ is not renormalized, as it is required by the condition that the electric charge is a conserved quantity [45]. Solving these equations and using $l = \log(\Lambda/E)$ we obtain $v(E)$, $A(E)$, and $Z(E)$ at energy E in the form

$$\frac{v(E)}{v} = \left(\frac{\Lambda}{E}\right)^{\gamma_v}, \frac{A(E)}{A} = \left(\frac{\Lambda}{E}\right)^{\gamma_A}, Z(E) = \left(\frac{\Lambda}{E}\right)^{-\gamma_z + \frac{\sqrt{15}}{\pi^{3/2}} \frac{\gamma_v}{N} l}. \quad (8)$$

We verified that same results are obtained by using the Wilsonian shell RG [43]. The analysis of Eq. (8) shows that there are three energy scales characterizing the system's behavior. At high energies, $E > E_1 = \Lambda e^{-b_1 N/\log N}$, where $b_1 = O(1)$, the dependence of the fermionic propagator on E is weak, i.e., fermions behave as almost free quasiparticles. At $E_2 < E < E_1$, where $E_2 = \Lambda e^{-b_2 N}$, $b_2 = O(1)$, v and A remain close to their bare values, but the quasiparticle residue becomes strongly E-dependent, and the fermionic propagator at the typical energy E acquires a non-Fermi-liquid form with anomalous exponent γ_z, i.e., $G \propto 1/E^{1-\gamma_z}$. This behavior holds also at energies below E_2, but now v and A grow as powers of Λ/E with anomalous exponents γ_v and γ_A, respectively. The presence of anomalous dimensions in the theory implies that physical observables, such as the specific heat, the compressibility, the diamagnetic susceptibility, etc., show unusual temperature dependencies, as shown below.

The strong coupling results differ only quantitatively from the case of graphene. In both cases, Coulomb interaction gives rise to anomalous exponents for the quasiparticle residue and the fermionic dispersion.

Weak coupling limit. The behavior described by Eq. (8) holds as long as the dressed dimensionless coupling $\alpha_N = (gZ)^2 N/v$ remains large. The bare value of α_N is of order N, however $v(E)$ grows upon the flow towards lower energies, and eventually, at $E < E_3 = \Lambda/N^N$, the dimensionless coupling α_N becomes smaller than one. Once this happens, the RG equations have to be modified because, e.g., bare $|q_x|$ in the bosonic propagator becomes larger than the $|q_x|$ term in the polarization operator. We evaluated the one-loop self-energy

and vertex corrections at small α_N and found that they are again logarithmical, but the RG parameter l is now $l = \log(E_m/E)$, where $E_m = g^2N^2/A$ is the energy scale below which the $\sqrt{|q_y|}$ term in the polarization dominates over the bare term $|q_y|$ in the boson propagator. The prefactors γ_z, γ_v and γ_A are different from those in Eq. (5) and are given by

$$\gamma_z = \frac{3\alpha_N}{8\pi^2 N},\ \gamma_v = \frac{\alpha_N}{4\pi^2 N},\ \gamma_A = \frac{\alpha_N |\log \alpha_N|}{2\pi^2 N}, \qquad (9)$$

Because $\alpha_N = Ng^2/v$, the factor N formally disappears from (9), but we recall that weak coupling approach is valid as long as $\alpha_N \leq 1$, hence α_N/N is still small in $1/N$. Note that argument of the logarithm in γ_A contains the coupling constant rather than the running energy, hence it changes the form of the β function, but does not invalidate one-loop RG. Performing the same RG analysis as in the strong coupling limit, we find that $Z(l)$, $v(l)$, and $A(l)$ still satisfy RG equations (7), but with γ's from Eq. (9). Solving these equations we obtain at smallest energies (largest l)

$$v(l) = \frac{g^2}{4\pi^2} l,\ Z(l) = l^{-3/2},\ A(l) = Ae^{\log^2 l}. \qquad (10)$$

We see that the quasiparticle Z does not reduce to a constant in the limit $\alpha_N \to 0$ but keeps decreasing, even at the smallest E. At the same time, we see that the series of logarithms at weak coupling do not generate anomalous dimensions, i.e., $v(l)$ and $Z(l)$ behave as powers of l (the inverse mass A has a somewhat more complex dependence on l, but still there is no anomalous dimension.) The logarithmic form of $Z(l)$ implies that the fermionic Green's function at the smallest energies behaves as $G(E) \sim (\log E)^{-3/2}/E$. Such behavior is generally termed as MFL. The outcome is that the weak coupling behavior of AWF is *qualitatively* different from that in graphene. In graphene, the quasiparticle Z factor tends to a finite value at zero energy [21], i.e. the system retains Fermi-liquid behavior with well defined quasiparticles. AWF, on the contrary, do not become sharp quasiparticles, even at the lowest energies.

To verify our analytical analysis, we obtained the RG flow of Z, $\alpha_N \propto 1/v$, and $1/A$ numerically for $N = 4$. (See Fig. 3.) We clearly see that v and A increase upon the system flows to lower energies (higher l), whereas the quasiparticle residue Z decreases, initially by a power law, and then nearly flattens at the largest l.

Physical observables. The non-trivial flow of v, A, and Z leads to rather non-trivial scaling relations for physical observables [22]. We present the calculations in SM and here list the results. At strong coupling the compressibility $\kappa = \frac{\partial n}{\partial \mu} \propto T^{1/2+\phi}$, the heat capacity $C \propto T^{\frac{3}{2}+\phi}$, and the diamagnetic susceptibility $\chi_{\rm dia} \propto -T^{-\frac{1}{2}-\phi}$, where $\phi = \gamma_v + \frac{1}{2}\gamma_A \approx 0.4255/N$ (see also Ref. [22]). The optical conductivity $\sigma_\alpha(\omega)$ in the strong coupling regime

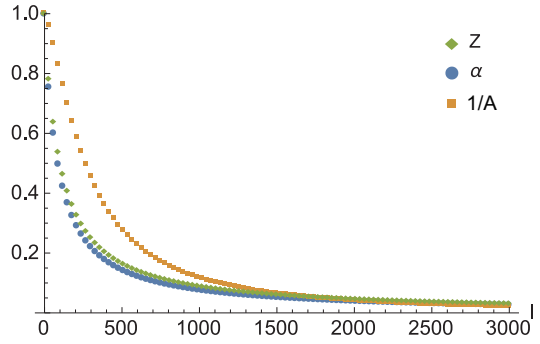

FIG. 3: (Color online) RG flow of the coupling constant $\alpha \propto 1/v$, the effective mass $1/A$, and the quasiparticle residue Z for 2D AWF. We set the initial values $\alpha_N = 4$ and $A = 1$ and the number of flavors $N = 4$. α, $1/A$, Z all flow to zero. The quasiparticle residue has power-law dependence $Z(E) \propto E^a$ at intermediate energies, typical for a non-Fermi liquid, and scales as $Z(E) \propto (1/|\log E|)^{3/2}$ at the lowest energies, i.e., at vanishing E the system displays MFL behavior.

is

$$\sigma_{x,y}(\omega) \propto N\frac{e^2}{\hbar}\left(\frac{\omega}{\omega_0}\right)^{\pm\left(\frac{1}{2}+\phi_\sigma\right)} \qquad (11)$$

where $\phi_\sigma = \gamma_v - \gamma_A/2 \approx 0.299/N$ and $\omega_0 = v^2/A$. The conductivity is anisotropic already for non-interacting AFW, however the anisotropy is amplified by interactions. In the weak-coupling regime

$$\sigma_{x,y}(\omega) \propto N\frac{e^2}{\hbar}\left(\frac{\omega e^{\log^2 \log \frac{\Lambda}{\omega}}}{\omega_0 \log^2 \frac{\Lambda}{\omega}}\right)^{\pm\frac{1}{2}}. \qquad (12)$$

Discussion and conclusion. In this paper we studied quantum critical behavior of 2D AWF with long-range Coulomb interaction. We performed RG analysis and demonstrated that interacting 2D AWFs display non-Fermi liquid behavior at intermediate energies, with various anomalous physical properties, and MFL behavior at the smallest energies.

There are several candidate materials for 2D AWFs. In deformed graphene [30–32] and pressured organic conductor α-(BEDT-TTF)$_2$I$_3$ [46], 2D AWFs emerge via the merging of two Dirac points. In TiO_2/VO_2 nanostructures 2D AWFs were predicted to be intrinsic low energy excitations due to the peculiar symmetry of the system [34–38]. 2D AWFs were also predicted theoretically to exist under external electric field or strain in black phosphorous (a system with a few layers of phosphorene) [33, 47], and this has been confirmed in a recent angle-resolved photo-emission study [48]. Furthermore, in some candidate systems the bare coupling constant α_N is not small [41]. For instance, in VO_2, $\alpha_N \approx 1.64$ based on $\varepsilon \approx 36$ [49], $v_F = 1.5 \times 10^5$ m/s [34], and $N = 4$ [36]. In black phosphorus, $\alpha_N = 0.88$ based on $\varepsilon \approx 10$ [50], $v_F = 5.0 \times 10^5$ m/s, and $N = 2$ [48].

If experimentalists succeed to fabricate freely suspended structures and tune them to the quantum-critical point, the effective coupling constant could be 10 times bigger, as in the case of graphene, what makes these structures likely candidate to observe the strong coupling behavior.

B.-J. Y and N. N. were supported by a Grant-in-Aid for Scientific Research on Innovative Areas "Topological Materials Science" (KAKENHI Grant No. 15H05853) and Kiban S Emergent electromagnetism in magnets (KAKENHI Grant No. 24224009). H. I. was supported by a Grant-in-Aid for JSPS Fellows. A. C was supported by the DOE grant DE-SC0014402, and J.S. is supported by the Deutsche Forschungsgemeinschaft through grant SCHM 1031/4-1.

Note added. On completion of our work, we became aware of a related work by G. Y. Cho and E.-G. Moon [53]. They studied the same model as we but employed different approximations and reached different conclusions. We compare our and their results in the SM [40].

[1] M. Z. Hasan and C. L. Kane, Rev. Mod. Phys. **82**, 3045 (2010).

[2] X. L. Qi and S. C. Zhang, Rev. Mod. Phys. **83**, 1057 (2011).

[3] X. Wan, A. M. Turner, A. Vishwanath, and S. Y. Savrasov, Phys. Rev. B **83**, 205101 (2011).

[4] S. Matsuura, P. Y. Chang, A. P. Schnyder, and S. Ryu, New J. Phys. **15**, 065001 (2013).

[5] Y. X. Zhao and Z. D. Wang, Phys. Rev. Lett. **110**, 240404 (2013).

[6] Y. X. Zhao and Z. D. Wang, Phys. Rev. B **89**, 075111 (2014).

[7] C. K. Chiu and A. P. Schnyder, Phys. Rev. B **90**, 205136 (2014).

[8] T. Morimoto and A. Furusaki, Phys. Rev. B **89**, 235127 (2014).

[9] B.-J. Yang and N. Nagaosa, Nat. Commun. **5**, 4898 (2014).

[10] B.-J. Yang, T. Morimoto and A. Furusaki, Phys. Rev. B **92**, 165120 (2015).

[11] A. A. Burkov, M. D. Hook, and Leon Balents, Phys. Rev. B **84**, 235126 (2011); D. A. Pesin and L. Balents, Nature Phys. **6**, 376 (2010).

[12] S. Murakami and S. -i. Kuga, Phys. Rev. B **78**, 165313 (2008); S. Murakami, New J. Phys. **9**, 356 (2007). In principle, chiral symmetry breaking can be also induced by interactions: D. V. Khveshchenko, Phys. Rev. Lett. **87**, 246802 (2001); E. V. Gorbar, V. P. Gusynin, V. A. Miransky, and I. A. Shovkovy, Phys. Rev. B **66**, 045108 (2002).

[13] B.-J. Yang, M. S. Bahramy, R. Arita, H. Isobe, E.-G. Moon, and N. Nagaosa, Phys. Rev. Lett. **110**, 086402 (2013).

[14] B.-J. Yang, E.-G. Moon, H. Isobe, and N. Nagaosa, Nature Phys. **10**, 774 (2014).

[15] B. Dóra, I. F. Herbut, and R. Moessner, Phys. Rev. B **88**, 075126 (2013).

[16] H.-H. Lai, Phys. Rev. B **91**, 235131 (2015); S.-K. Jian and H. Yao, Phys. Rev. B **92**, 045121 (2015).

[17] A. H. Castro Neto, F. Guinea, N. M. R. Peres, K. S. Novoselov, A. K. Geim, Rev. Mod. Phys. **81**, 109 (2009).

[18] D. M. Basko and I. L. Aleiner, Phys. Rev. B **77**, 041409(R) (2008); M. S. Foster and I. L. Aleiner, Phys. Rev. B 77, 195413 (2008); V. Juricic, O. Vafek, and I. F. Herbut, Phys. Rev. B **82**, 235402 (2010); M. A. H. Vozmediano and F. Guinea, Phys. Scr. **T146** 014015 (2012); Y. Lemonik, I. L. Aleiner, V. I. Fal'ko Phys. Rev. B **85**, 245451 (2012); O. Vafek and A. Vishwanath, Annu. Rev. Condens. Matter Phys. **5**, 83 (2014); J. M. Murray and O. Vafek, Phys. Rev. B **89**, 201110 (2014).

[19] J. González, F. Guinea and M. A. H. Vozmediano, Nucl. Phys. B **424**, 595 (1994).

[20] D. T. Son, Phys. Rev. B **75**, 235423 (2007).

[21] The quasiparticle residue Z in graphene is studied in many papers, e.g., J. González, F. Guinea, and M. A. H. Vozmediano, Phys. Rev. B **59**, R2474 (1999); E. Barnes, E. H. Hwang, R. E. Throckmorton, and S. Das Sarma, Phys. Rev. B **89**, 235431 (2014). Some earlier papers refer to graphene as a MFL. We, however, use stricter definition of MFL, namely we call the behavior MFL when the quasiparticle residue Z vanishes logarithmically as $\omega \to 0$.

[22] D. E. Sheehy and J. Schmalian, Phys. Rev. Lett. **99**, 226803 (2007).

[23] I. F. Herbut, V. Juricic, O. Vafek, Phys. Rev. Lett. **100**, 046403 (2008).

[24] P. Goswami and S. Chakravarty, Phys. Rev. Lett. **107**, 196803 (2011).

[25] P. Hosur, S. A. Parameswaran, and A. Vishwanath, Phys. Rev. Lett. **108**, 046602 (2012).

[26] H. Isobe and N. Nagaosa, Phys. Rev. B **86**, 165127 (2012).

[27] H. Isobe and N. Nagaosa, Phys. Rev. B **87**, 205138 (2013).

[28] E. G. Mishchenko, Europhys. Lett. **83**, 17005 (2008).

[29] D. E. Sheehy and J. Schmalian, Phys. Rev. B **80**, 193411 (2009)

[30] G. Montambaux, F. Piechon, J.-N. Fuchs, and M. O. Goerbig, Eur. Phys. J. B **72**, 509 (2009).

[31] G. Montambaux, F. Piechon, J.-N. Fuchs, and M. O. Goerbig, Phys. Rev. B **80**, 153412 (2009).

[32] P. Dietl, F. Piéchon, and G. Montambaux, Phys. Rev. Lett. **100**, 236405 (2008).

[33] M. Ezawa, New J. Phys. **16**, 115004 (2014).

[34] V. Pardo and W. E. Pickett, Phys. Rev. Lett. **102**, 166803 (2009).

[35] V. Pardo and W. E. Pickett, Phys. Rev. B **81**, 035111 (2010).

[36] S. Banerjee, R. R. P. Singh, V. Pardo, and W. E. Pickett, Phys. Rev. Lett. **103**, 016402 (2009).

[37] P. Delplace and G. Montambaux, Phys. Rev. B **82**, 035438 (2010).

[38] S. Banerjee and W. E. Pickett, Phys. Rev. B **86**, 075124 (2012).

[39] B. L. Altshuler, L. B. Ioffe, and A. J. Millis, Phys. Rev. B **50**, 14048 (1994); J. Polchinski, Nucl. Phys. B **422**, 617 (1994); Ar. Abanov, A. V. Chubukov, and J. Schmalian, Adv. Phys. **52** 119 (2003); M. A. Metlitski and S. Sachdev, Phys. Rev. B, **82**, 075128 (2010); D. F. Mross, J. McGreevy, H. Liu, and T. Senthil, Phys. Rev. B **82**, 045121 (2010); K. B. Efetov, H. Meier and

C. Pépin, Nature Phys. **9** 442, (2013); A. V. Chubukov and P. Wölfle, Phys. Rev. B, **89**, 045108 (2014). For alternative approach, see A. L. Fitzpatrick, S. Kachru, J. Kaplan, and S. Raghu, Phys. Rev. B **89**, 165114 (2014), and references therein. Problems with $1/N$ expansion at higher-loop order due to special role of forward and backward scattering for fermions with a full 2D Fermi surface have been first reported by S.S. Lee, Phys. Rev. B **80**, 165102 (2009).

[40] See Supplemental Material for the derivations of the one-loop polarization $\Pi_1(\Omega, \boldsymbol{q})$ and self-energy $\Sigma_1(\omega, \boldsymbol{k})$, screening of a charged impurity, the physical observables, and detailed explanations for the theory, which includes Refs. [51–53].

[41] Such an anisotropic momentum dependence of the polarization function can induce a highly anisotropic distribution of screening charges once a charged impurity is introduced to the system (see SM [40] for details).

[42] A. A. Abrikosov, L. P. Gorkov, and I. E. Dzyaloshinski, Methods of quantum field theory in statistical physics, (Dover Publications, New York, 1963); E. M. Lifshitz and L. P. Pitaevski, Statistical Physics, (Pergamon Press, 1980). For recent analysis how singular terms in $\Pi(\Omega, \mathbf{q})$ affect thermodynamics see D. Belitz, T. R. Kirkpatrick, and T. Vojta, Rev. Mod. Phys. **77**, 579 (2005); H. v. Löhneysen, A. Rosch, M. Vojta, and P. Wolfle, Rev. Mod. Phys. **79**, 1015 (2007); D. L. Maslov and A. V. Chubukov, Phys. Rev. B **81**, 045110 (2010).

[43] R. Shankar, Rev. Mod. Phys. **66**, 129 (1994).

[44] See, e.g., K. Le Hur and T.M. Rice, Ann. Phys. **324**, 1452 (2009).

[45] In our diagrammatic approach, g is defined as the full vertex, and thus it is renormalized as $1/Z$ such that $g * Z$ remains a constant. The Wilsonian RG approach uses the quantity gZ as the vertex "g", which is associated with the electric charge and is not renormalized. This is just the issue of different nomenclature used in the two different RG approaches for the RG analysis, the final results are indeed the same. We discuss this issue in more detail in the SM [40].

[46] S. Katayama, A. Kobayashi, Y. Suzumura, J. Phys. Soc. Jpn. **75**, 054705 (2006); A. Kobayashi, S. Katayama, Y. Suzumura, H. Fukuyama, J. Phys. Soc. Jpn. **76**, 034711 (2007); M. O. Goerbig, J.-N. Fuchs, G. Montambaux, and F. Piéchon, Phys. Rev. B **78**, 045415 (2008).

[47] Q. Liu, X. Zhang, L. B, Abdalla, A.Fazzio, and A. Zunger, Nano Lett. **15**, 1222 (2015); K. Dolui and S. Y. Quek, arXiv:1503.03647; Z. J. Xiang, G. J. Ye, C. Shang, B. Lei, N. Z. Wang, K. S. Yang, D. Y. Liu, F. B. Meng, X. G. Luo, L. J. Zou, Z. Sun, Y. B. Zhang, and X.H. Chen, arXiv:1504.00125; P. -L. Gong, D. -Y. Liu, K. -S. Yan, Z. -J. Xiang, X. -H. Chen, S. -Q. Shen, and L.-J. Zou, arXiv:1507.03213.

[48] J. Kim, S. S. Baik, S. H. Ryu, Y. Sohn, S. Park, B.-G. Park, J. Denlinger, Y. Yi, H. J. Choi, and K. S. Kim, Science **349**, 723 (2015).

[49] Z. Yang, C. Ko, V. Balakrishnan, G. Gopalakrishnan, and S. Ramanathan, Phys. Rev. B **82**, 205101 (2010).

[50] T. Nagahama, M. Kobayashi, Y. Akahama, S. Endo, and S.-i. Narita, J. Phys. Soc. Jpn. **54**, 2096 (1985).

[51] C. M. Varma, P. B. Littlewood, S. Schmitt-Rink, E. Abrahams, and A. E. Ruckenstein, Phys. Rev. Lett. **63**, 1996 (1989).

[52] J. González, F. Guinea, and M. A. H. Vozmediano, Phys. Rev. B **59**, R2474 (1999).

[53] G. Y. Cho and E.-G. Moon, arXiv:1508.03777.